Cognitive Non-Orthogonal Multiple Access with Cooperative Relaying and Antenna Optimization using SADEA for Efficient Spectrum Sharing

Yohane Joseph Ntonya
Department of Electrical Engineering, Pan African University Institute for Basic Sciences and Technology and Innovation, Nairobi, Kenya
yohane.joseph@students.jkuat.ac.ke (corresponding author)

Stephen Musyoki
Department of Electrical Engineering, Technical University of Kenya, Kenya
Smusyoki@yahoo.com

Vitalice Oduol
Department of Electrical Engineering, University of Nairobi, Kenya
vitalice.oduol@gmail.com

Received: 16 January 2025 | Revised: 15 February 2025 | Accepted: 6 March 2025

 DOI: https://doi.org/10.48084/etasr.10265

ABSTRACT

With the escalating need for efficient spectrum utilization, creative solutions are needed to enhance system performance in 5G wireless networks. This study presents a novel Cognitive Non-Orthogonal Multiple Access (C-NOMA) system coupled with cooperative relaying enhanced by Surrogate Model-Assisted Differential Evolution for Antenna Synthesis (SADEA) for antenna optimization. Latency, spectral efficiency, antenna parameters, and design protocols are studied to optimize the antenna and design protocol to reduce Outage Probability (OP) and Bit Error Rate (BER). The proposed method uses Probability Density Functions (PDF) for Rayleigh fading channels to derive system performance equations, evaluate metrics such as OP and BER, and finally perform MATLAB-based simulations. Robust signal processing is also ensured by Successive Interference Cancellation (SIC) and Channel State Information (CSI) techniques. The proposed SADEA-optimized system showed superior results to conventional methods, providing better BER and OP for communication reliability for 64 QAM and 128 QAM modulation schemes, for various SNR values and path numbers (*L*). The inclusion of SADEA in C-NOMA systems represents a promising avenue to achieve spectrum sharing and optimization of system performance in 5G networks.

Keywords-SADEA; cooperative relaying; decode and forward relay; interference mitigation; modulation scheme; Non-Orthogonal Multiple Access (NOMA)

I. INTRODUCTION

The dynamic evolution of wireless communication demands efficient spectrum utilization [1], especially in fifth-generation (5G) networks [2]. These networks aim to provide enhanced data rates, ultra-low latency, and massive connectivity for applications such as IoT, autonomous vehicles, and smart cities [3-5]. Achieving these goals requires innovative approaches to address spectrum scarcity, interference management, and resource allocation challenges [6]. Non-Orthogonal Multiple Access (NOMA) improves spectral efficiency by allowing simultaneous data transmission [7] through power-domain multiplexing and Successive Interference Cancellation (SIC) [8-9]. Cognitive Radio (CR) further enhances NOMA by allowing dynamic spectrum access and reducing interference between primary and secondary users [10-11]. Integrating Cognitive NOMA (C-NOMA) with cooperative relaying enhances spectrum-sharing efficiency in 5G [12-13].

Antenna optimization plays a crucial role in maximizing system performance in Rayleigh fading environments [14-16]. This study leverages Surrogate Model-Assisted Differential Evolution for Antenna Synthesis (SADEA), integrating

machine learning into evolutionary computation for robust optimization [17-20]. SADEA enables optimal antenna configurations, minimizing Outage Probability (OP) and Bit Error Rate (BER), thus improving system reliability [21-22].

Several studies have highlighted the transformative potential of NOMA. In [24], C-NOMA designs with cooperative relaying were analyzed. In [25], NOMA was explored for airborne base stations, while Rate Splitting Multiple Access (RSMA) was examined in [26]. Other research on MIMO-NOMA [28-34] and RIS-NOMA [29] emphasized enhanced spectral efficiency and reliability. This study addresses key challenges in spectrum sharing, system reliability, and antenna design for 5G networks. Contributions include optimized antenna design using SADEA for cost-effective synthesis, and enhanced spectrum efficiency through C-NOMA and cooperative relaying.

II. METHODOLOGY

This section describes an overall approach to designing and evaluating the C-NOMA system, exploiting a cooperative relay and antenna design that will maximize spectrum-sharing efficiency.

A. Cognitive-NOMA (C-NOMA) System Network Model Analysis

The proposed C-NOMA system consists of a Base Station (BS), two Users (U_1 and U_2), and L intermediate Decode and Forward (DF) relay nodes. In this system, the Primary User (PU) represents the licensed user with priority spectrum access, while the Secondary User (SU) opportunistically accesses the spectrum under cognitive radio constraints. The relays enhance communication by assisting both users while mitigating interference. Figure 1 presents a C-NOMA system, illustrating the interaction between the BS, relays, and users. The users employ higher-order MQAM for spectral efficiency and robustness. The wireless channels follow Rayleigh fading, which accurately models real-world wireless conditions, particularly in urban environments with multipath propagation [28]. Each node operates in half-duplex mode with a single antenna, and Channel State Information (CSI) is assumed to be imperfect, impacting the decoding process.

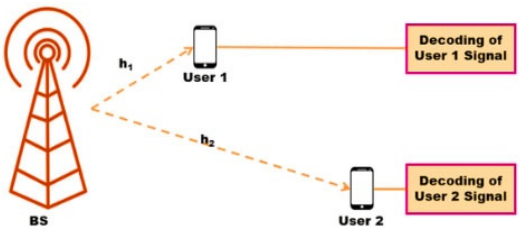

Fig. 1. The C-NOMA system.

The BS transmits a Superposition-Coded (SC) signal comprising messages M_1 and M_2 for U_1 and U_2, respectively. Since U_2 has a better channel gain than U_1 $\left(\left|h_{U_2}\right|^2 > \left|h_{U_1}\right|^2\right)$, power allocation follows NOMA principles, where U_1 is assigned a higher power fraction due to its weaker channel conditions. The received SC signal at a relay node R_L can be expressed as:

$$Y_{R_L} = \left(\sqrt{P_{L-1}\beta_1}M_1 + \sqrt{P_{L-1}\beta_2}M_2\right)\left(\hat{h}_{R_L} + k\right) + n_{R_L} \quad (1)$$

where $\beta_1 > \beta_2$ are power allocation coefficients and $\beta_1 + \beta_2 = 1$, P_{L-1} is the transmit power at relay R_L, $\hat{h}_{R_L}$ is the estimated channel coefficient, k is the channel estimation error, and n_{R_L} is the Additive White Gaussian Noise (AWGN).

At the user end, U_1 detects M_1 by treating M_2 as noise, while U_2 applies SIC to decode M_1 first and then extract M_2. The received signal at U_i is given by:

$$Y_{U_i} = \left(\sqrt{P_L\beta_1}M_1 + \sqrt{P_L\beta_2}M_2\right)\left(\hat{h}_{U_i} + k\right) + n_{U_i} \quad (2)$$

where P_L is the transmit power at the last relay, and n_{U_i} is AWGN at U_i. This model allows efficient spectrum utilization, balancing PU priority access with SU opportunistic transmission while ensuring robust communication via cooperative relaying and SIC. Figure 2 shows a flowchart of the system.

B. Optimization of the Transmitting Antenna Using SADEA

This study utilized the Bowtie Dipole antenna, as described in [35], at the transmitter, and the antenna was optimized using SADEA. The SADEA optimization method was employed for optimizing three different antenna structures, labeled A1 to A3. SADEA is employed to optimize key parameters of the Bowtie Dipole antenna, including arm length, flare angle, and the separation gap between the antenna and the dielectric. The goal is to enhance coupling between antennas A2 and A3 while minimizing crosstalk from A1.

For implementation, the optimization process uses the Differential Evolution (DE) algorithm as its search method, while the Gaussian Process (GP) was used for surrogate modeling. Figures 3 and Figure 4 illustrate the fundamental and parametrized design of the isosceles triangle Bowtie antenna, which has a total length of 0.2385λ and a width of 0.1073λ. The dielectric material associated with this design features a length of 1.66λ, a width of 1.25λ, and a thickness of 0.833λ. These values are determined based on the central frequency, with a relative permittivity (ε_r) of 5 and conductivity (σ) of 0.1, aligning with the electrical properties of standard concrete utilized within the hybrid domain of the total far-field region. To assess performance variations, the separation distance between the antenna and the dielectric was set at 10, 20, and 30 mm.

The primary goal of the optimization process is to enhance the coupling between antennas A2 and A3 while simultaneously minimizing crosstalk from antenna A1. This optimization problem is mathematically formulated as:

$$f(x) = \begin{cases} maximize & coupling(A2, A3) \\ s.t. & crosstalk(A1, A2) \leq 45dB \end{cases} \quad (3)$$

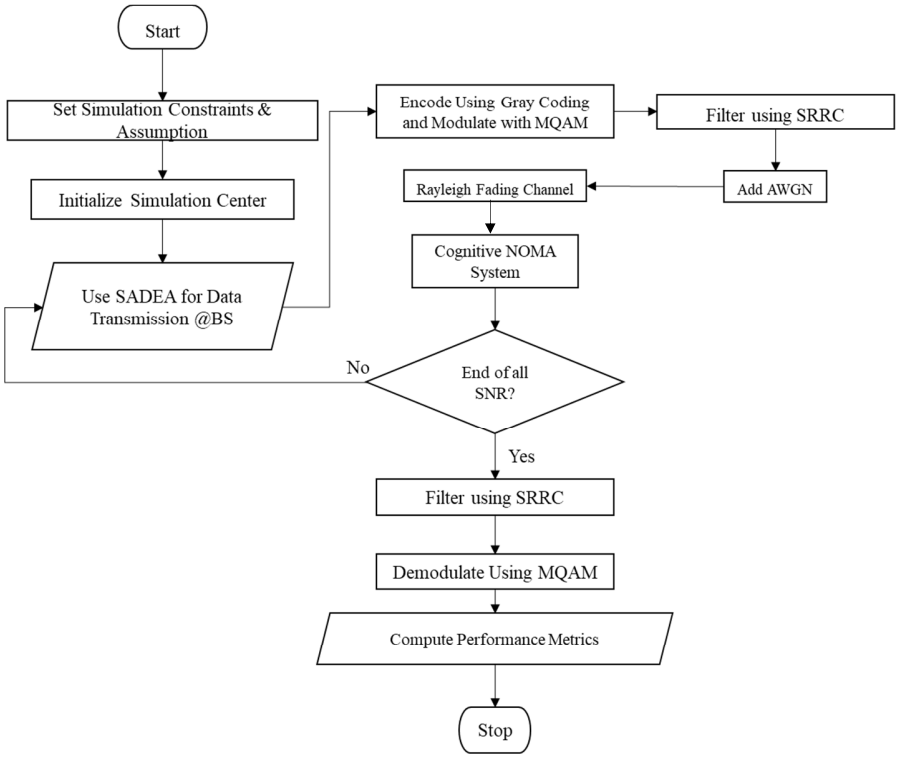

Fig. 2. Flowchart of the proposed C-NOMA.

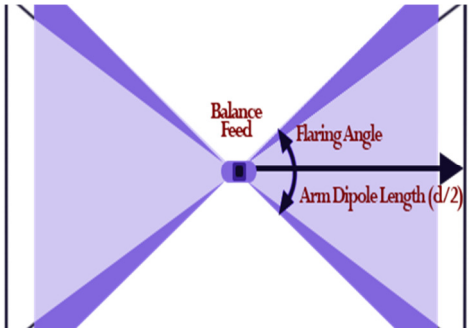

Fig. 3. Bowtie antenna geometry.

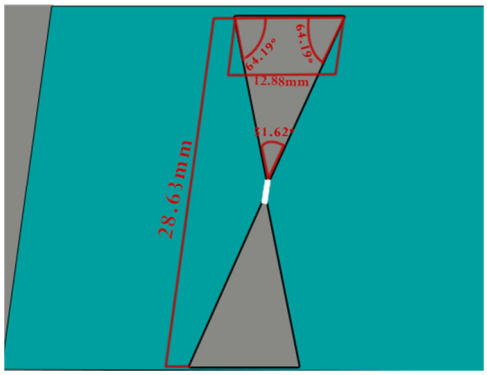

Fig. 4. Bowtie antenna parametric design of the isosceles triangle.

To facilitate optimization, SADEA maintains a database that stores precisely evaluated solutions along with their respective function values, allowing the process to be streamlined. When a new function x is assessed, the database is updated with the corresponding exact function value. The initial sampling process is executed using Latin Hypercube Sampling (LHS), which provides a well-distributed sample set across the design space. This sampling approach improves efficiency by requiring fewer samples while still achieving comprehensive coverage. The SADEA optimization process follows a structured implementation, illustrated in Figure 5.

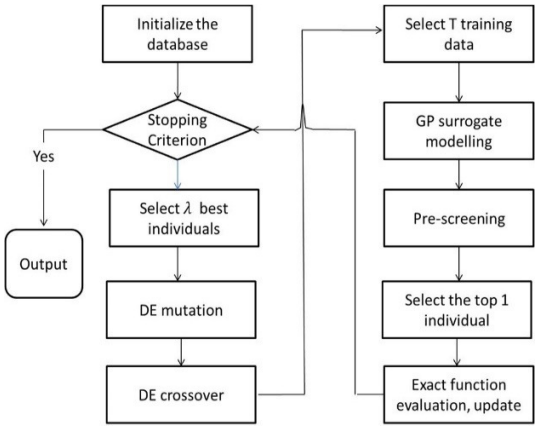

Fig. 5. Flowchart of SADEA optimization process.

The optimized antenna performance is further analyzed by return loss measurements. Parameterized return loss is observed at the input port for varying values of k within the

range of 0-14 mm, with the reflection coefficient for different antenna arm lengths represented along the vertical axis. For the SADEA-based optimization process, an initial set of 40 samples is established to accommodate the configuration of 10 design variables. The remaining parameters are detailed in Table I. The optimization achieved an improved bandwidth of 618 MHz, and the optimization refines the coupling between antennas A2 and A3, achieving a value of -18.25 dB while ensuring that the crosstalk remains within the acceptable limit of -36.23 dB. Each candidate solution requires approximately 6 minutes for a complete evaluation in this optimization framework. The primary objective is to achieve impedance matching over a broad frequency range (1-4 GHz). The SADEA algorithm effectively identifies optimal design parameters that provide the best matching across a bandwidth of 3.25 GHz. The optimization process reaches convergence at an iteration count of approximately 450.

III. PERFORMANCE METRICS

The effectiveness of the proposed C-NOMA system was assessed using two key metrics: BER and OP. BER quantifies the reliability of data transmission by measuring the frequency of bit errors, while OP determines the likelihood that the system's Signal-to-Noise Ratio (SNR) falls below a critical threshold, leading to communication failure. These metrics collectively evaluate the accuracy and robustness of the proposed approach.

A. Bit Error Rate (BER)

The BER was derived for users U_1 and U_2 under both perfect and imperfect SIC and CSI conditions. At U_1, Maximum Likelihood Detection (MLD) was applied, where detection errors arose due to channel estimation inaccuracies. At U_2, SIC was employed to decode symbols sequentially, and the BER was analyzed under two conditions: when the primary symbols were correctly detected and when detection errors propagated through SIC. Thus, the BER for U_i is determined by:

$$BER_{\mathrm{U}_i} = \frac{1}{2}\Big[P\left(\left(\sqrt{P_L\beta_1}+\sqrt{P_L\beta_2}\right)\hat{h}_{\mathrm{U}_i} < \left(\sqrt{P_L\beta_1}+\sqrt{P_L\beta_2}\right)k + n_{\mathrm{U}_i}\right) + P\left(\left(\sqrt{P_L\beta_1}-\sqrt{P_L\beta_2}\right)\hat{h}_{\mathrm{U}_i} < \left(\sqrt{P_L\beta_1}-\sqrt{P_L\beta_2}\right)k + n_{\mathrm{U}_i}\right)\Big] \quad (4)$$

B. Outage Probability (OP)

The OP was evaluated by determining the probability that the received SNR at U_1 and U_2 dropped below predefined thresholds. At U_1, OP was derived under imperfect CSI conditions, considering direct detection failures. At U_2, OP was calculated as a combination of two cases: when the SIC process failed for primary symbols and when the direct decoding of secondary symbols was unsuccessful. Thus, the OP for U_i is:

$$P_{out,\,U_i} = 1 - exp\left(-\frac{\lambda_i^{th}\left(P_L\sigma_{U_i}^2+\varrho_{U_i}^2\right)}{\left(P_L\beta_1-\lambda_i^{th}P_L\beta_2\right)\widehat{\omega}_{U_i}}\right) \quad (5)$$

where $\widehat{\omega}_{U_i} = E\left[\left|\hat{h}_{\mathrm{U}_i}\right|^2\right]$, and $\lambda_i^{th} = 2^{(L+1)T} - 1$ is the threshold.

IV. RESULTS AND DISCUSSION

This section delves into the analysis of BER and OP for the developed system compared to the conventional system. The performance metrics were evaluated across various SNR levels, modulation schemes, and path numbers.

A. Bit Error Rate

The BER results for both 64-QAM and 128-QAM modulation schemes at different numbers of paths (L) and varying SNRs were obtained from a MATLAB simulation. For 64-QAM, the BER decreases consistently with increasing SNR and is influenced by the number of relay paths. At L=2, the BER decreases from 7.77647×10^{-5} at 0 dB to 5.42×10^{-8} at 20 dB. For L=3, the BER starts at 8.3441×10^{-6} at 0 dB and reduces to 5.8×10^{-9} at 20 dB. Similarly, at L=4, the BER drops from 9.799×10^{-7} at 0dB to 7×10^{-10} at 20 dB.

Simulation using 128-QAM also showed a similar trend. At L=2, the BER starts at 0.001232588 at 0 dB and decreases to 8.588×10^{-7} at 20 dB. For L =3, the BER drops from 0.000132211 at 0 dB to 9.22×10^{-8} at 20 dB. At L=4, the BER reduces from 1.55271×10^{-5} at 0 dB to 1.08×10^{-8} at 20 dB. These results comprehensively detail the BER performance across varying SNR and relay configurations.

B. Outage Probability (OP)

The OP results for both 64-QAM and 128-QAM modulation schemes across different numbers of paths (L) and varying SNRs were obtained from a simulation. For 64-QAM, the OP decreases consistently with increasing SNR and is influenced by the number of relay paths. At L=2, the OP drops from 0.002913368 at 0 dB to 0.000546421 at 20 dB. For L=3, the OP starts at 0.00023575 at 0 dB and decreases to 0.0000442164 at 20 dB. Similarly, for L=4, the OP decreases from 2.60581×10^{-5} at 0 dB to 4.8874×10^{-6} at 20 dB.

The 128-QAM modulation also follows a similar trend. At L=2, the OP starts at 0.008359316 at 0 dB and decreases to 0.001567842 at 20 dB. For L=3, it decreases from 0.000676436 at 0 dB to 0.000126869 at 20 dB. Finally, at L=4, the OP decreases from 7.47686×10^{-5} at 0dB to 1.40232×10^{-5} at 20 dB. These results highlight the detailed performance variations across modulation schemes, relay paths, and SNR.

C. Results' Benchmarking

BER results from the proposed system and the conventional system were compared, showing substantial performance improvement due to the use of SADEA. Figure 6, which compares 64-QAM BER results, clearly shows that the SADEA-enhanced system outperforms the conventional system across all SNR levels and numbers of paths (L). For instance, at L=2 and SNR = 20 dB, the BER of the SADEA-enhanced system is 5.42×10^{-8}, significantly lower than the conventional system's BER of 9.22×10^{-7}. This represents an improvement of approximately an order of magnitude. Similar trends are observed for L=3 and L=4. Figure 7 shows the BER performance for 128-QAM, where SADEA optimization yields even more pronounced benefits due to the higher complexity of this modulation. For L=2 and SNR = 20 dB, the BER of the SADEA-enhanced system is 8.588×10^{-7}, compared to $1.46\times10^{-}$

[5] for the conventional system. This improvement demonstrates the efficiency of SADEA in minimizing errors, particularly in high-complexity modulation schemes. The results highlight the critical role of SADEA in optimizing antenna parameters, reducing BER significantly, and enhancing overall system reliability in both low and high-complexity scenarios.

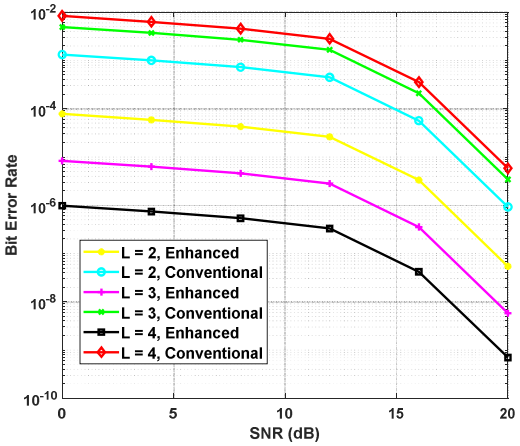

Fig. 6. BER comparison for 64-QAM.

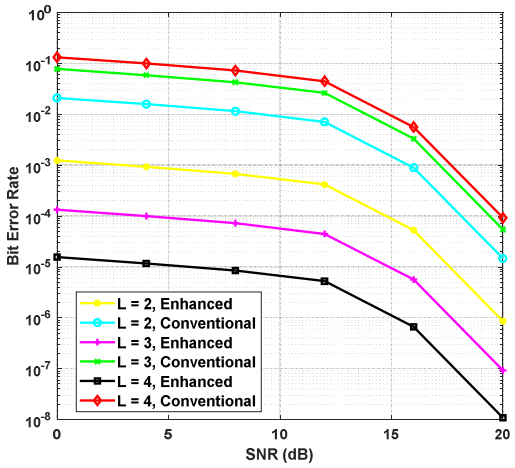

Fig. 7. BER graph comparison for 128-QAM.

The comparison of OP results between the SADEA-optimized system and the conventional system showcases a remarkable improvement in performance. As shown in Figure 8, the SADEA-enhanced system demonstrates significantly lower OP across all SNR values and path numbers (L). For instance, at L=2 and SNR = 0 dB, the OP of the SADEA system is just 0.00291, a drastic reduction compared to 0.05535 in the conventional system. This trend continues as SNR increases, highlighting the effectiveness of SADEA in improving reliability.

Similarly, the results for 128 QAM, shown in Figure 9, show an even larger performance gap. The SADEA-optimized system also outperforms the conventional systems at L=2 and SNR = 4 dB, with an OP of 0.00356, whereas the conventional system offers 0.06758. The improvement is consistent with increasing values of L and SNR for all values of L and SNR and is thus able to handle the greater SNR and L complexity present in the 128-QAM 2-bit symbol as well as maintain robust performance.

These results undoubtedly demonstrate how SADEA can effectively contribute to antenna parameter optimization, resulting in higher reliability and lower outage rates for the system. SADEA is shown to be a vital component in improving wireless communication systems by minimizing signal loss and improving transmission quality.

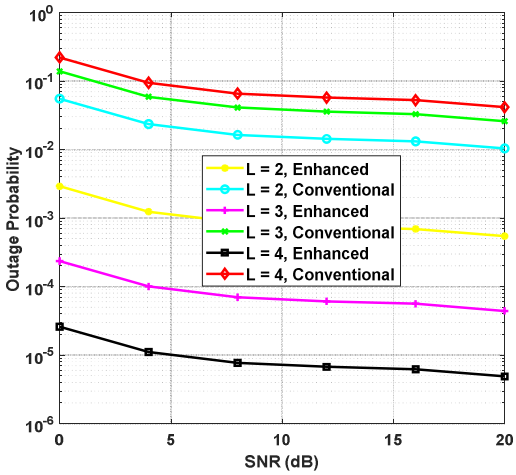

Fig. 8. OP comparison for 64-QAM.

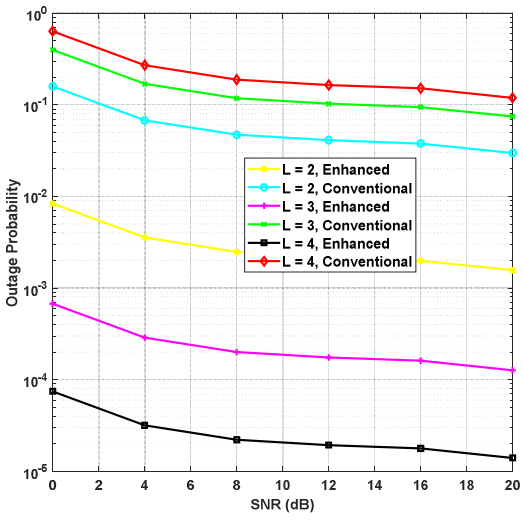

Fig. 9. OP comparison for 128-QAM.

V. CONCLUSION

The proposed system showed great improvement in primary key metrics, including BER, OP, and spectral efficiency. MATLAB simulations of the SADEA algorithm illustrated how antenna parameters could be optimized via the algorithm, reducing computational cost while providing superior performance across 64-QAM and 128-QAM modulation schemes. The proposed method was compared

favorably to conventional systems based on reliability, transmission quality, and resource efficiency. These results show that the proposed framework can address the challenges of 5G networks, paving the way for future applications in next-generation wireless communication systems with high spectral efficiency and low latency transmission.

ACKNOWLEDGMENT

The author expresses his profound appreciation to the African Union Organization and PAUSTI for the financial support provided to enable this research. Additionally, he expresses his gratitude to his supervisors, Professor Stephen Musyoki and Professor Vitalice Oduol, for their supervision and guidance throughout this work.

REFERENCES

[1] M. Ali, M. N. Yasir, D. M. S. Bhatti, and H. Nam, "Optimization of Spectrum Utilization Efficiency in Cognitive Radio Networks," *IEEE Wireless Communications Letters*, vol. 12, no. 3, pp. 426–430, Mar. 2023, https://doi.org/10.1109/LWC.2022.3229110.

[2] Z. Quan, S. Cui, and A. H. Sayed, "Optimal Linear Cooperation for Spectrum Sensing in Cognitive Radio Networks," *IEEE Journal of Selected Topics in Signal Processing*, vol. 2, no. 1, pp. 28–40, Feb. 2008, https://doi.org/10.1109/JSTSP.2007.914882.

[3] Y. Ji, J. Zhang, Y. Xiao, and Z. Liu, "5G flexible optical transport networks with large-capacity, low-latency and high-efficiency," *China Communications*, vol. 16, no. 5, pp. 19–32, May 2019, https://doi.org/10.23919/j.cc.2019.05.002.

[4] K. Arai and M. Murakami, "High-accuracy Time-synchronization Technology for Low-latency, High-capacity Communications in the 5G and Beyond 5G eras," *NTT Technical Review*, vol. 19, no. 12, pp. 85–92, Dec. 2021, https://doi.org/10.53829/ntr202112gls.

[5] S. Liu and D. Liu, "A High-Flexible Low-Latency Memory-Based FFT Processor for 4G, WLAN, and Future 5G," *IEEE Transactions on Very Large Scale Integration (VLSI) Systems*, vol. 27, no. 3, pp. 511–523, Mar. 2019, https://doi.org/10.1109/TVLSI.2018.2879675.

[6] M. U. A. Siddiqui, F. Qamar, F. Ahmed, Q. N. Nguyen, and R. Hassan, "Interference Management in 5G and Beyond Network: Requirements, Challenges and Future Directions," *IEEE Access*, vol. 9, pp. 68932–68965, 2021, https://doi.org/10.1109/ACCESS.2021.3073543.

[7] D. Sharma and D. Mousik, "A Study on Non-Orthogonal Multiple Access (NOMA) for 5G systems and beyond," *International Journal of Software & Hardware Research in Engineering*, vol. 8, no. 2, Feb. 2020, https://doi.org/10.26821/IJSHRE.8.2.2020.8206.

[8] M. Baghani, S. Parsaeefard, M. Derakhshani, and W. Saad, "Dynamic Non-Orthogonal Multiple Access and Orthogonal Multiple Access in 5G Wireless Networks," *IEEE Transactions on Communications*, vol. 67, no. 9, pp. 6360–6373, Sep. 2019, https://doi.org/10.1109/TCOMM.2019.2919547.

[9] M. Liaqat, K. A. Noordin, T. Abdul Latef, and K. Dimyati, "Power-domain non orthogonal multiple access (PD-NOMA) in cooperative networks: an overview," *Wireless Networks*, vol. 26, no. 1, pp. 181–203, Jan. 2020, https://doi.org/10.1007/s11276-018-1807-z.

[10] A. Ebrahim, A. Celik, E. Alsusa, M. W. Baidas, and A. M. Eltawil, "Hybrid Multiple-Access: Mode Selection, User Pairing and Resource Allocation," *IEEE Access*, vol. 11, pp. 107251–107264, 2023, https://doi.org/10.1109/ACCESS.2023.3320640.

[11] Y. Luo, C. Wu, Y. Leng, N. Huang, L. Mao, and J. Tang, "Throughput Optimization for NOMA Cognitive Relay Network with RF Energy Harvesting Based on Improved Bat Algorithm," *Mathematics*, vol. 10, no. 22, Nov. 2022, Art. no. 4357, https://doi.org/10.3390/math10224357.

[12] V. S. Nguyen and T. H. Nguyen, "Performance Analysis of Cognitive-Inspired Wireless Powered NOMA Systems With Joint Collaboration," *IEEE Access*, vol. 11, pp. 51578–51589, 2023, https://doi.org/10.1109/ACCESS.2023.3280049.

[13] H. Liu, Z. Ding, K. J. Kim, K. S. Kwak, and H. V. Poor, "Decode-and-Forward Relaying for Cooperative NOMA Systems With Direct Links," *IEEE Transactions on Wireless Communications*, vol. 17, no. 12, pp. 8077–8093, Dec. 2018, https://doi.org/10.1109/TWC.2018.2873999.

[14] K. Suriyan, R. Nagarajan, and G. Ghinea, "Smart Antenna Optimization Techniques for Wireless Applications," *Electronics*, vol. 12, no. 13, Jul. 2023, Art. no. 2983, https://doi.org/10.3390/electronics12132983.

[15] D. D. Devisasi Kala and D. T. Sundari, "A review on optimization of antenna array by evolutionary optimization techniques," *International Journal of Intelligent Unmanned Systems*, vol. 11, no. 1, pp. 151–165, Jan. 2023, https://doi.org/10.1108/IJIUS-08-2021-0093.

[16] Q. Wu, Y. Cao, H. Wang, and W. Hong, "Machine-learning-assisted optimization and its application to antenna designs: Opportunities and challenges," *China Communications*, vol. 17, no. 4, pp. 152–164, Apr. 2020, https://doi.org/10.23919/JCC.2020.04.014.

[17] M. Akinsolu, "Efficient Surrogate Model-Assisted Evolutionary Algorithm for Electromagnetic Design Automation with Applications," Ph.D. dissertation, University of Chester, UK, 2019.

[18] K. Fu, X. Cai, B. Yuan, Y. Yang, and X. Yao, "An Efficient Surrogate Assisted Particle Swarm Optimization for Antenna Synthesis," *IEEE Transactions on Antennas and Propagation*, vol. 70, no. 7, pp. 4977–4984, Jul. 2022, https://doi.org/10.1109/TAP.2022.3153080.

[19] A. Cordero-Samortin, J. D. Cruz, and Z. Mabunga, "The Optimization of a 5G Inset-fed Patch Antenna Using the Machine Learning Algorithm Surrogate Model Assisted Differential Evolution for Antenna Synthesis," in *2021 IEEE 4th International Conference on Computer and Communication Engineering Technology (CCET)*, Beijing, China, Aug. 2021, pp. 371–375, https://doi.org/10.1109/CCET52649.2021.9544345.

[20] M. O. Akinsolu, P. Excell, and B. Liu, "Surrogate Model-Assisted Global Optimization for Antenna Design," in *Surrogate Modeling for High-Frequency Design*, World Scientific (Europe), 2022, pp. 123–152.

[21] B. Liu, S. Koziel, and N. Ali, "SADEA-II: A generalized method for efficient global optimization of antenna design," *Journal of Computational Design and Engineering*, vol. 4, no. 2, pp. 86–97, Apr. 2017, https://doi.org/10.1016/j.jcde.2016.11.002.

[22] L. Yu, C. Ren, and Z. Meng, "A Surrogate-Assisted Differential Evolution with fitness-independent parameter adaptation for high-dimensional expensive optimization," *Information Sciences*, vol. 662, Mar. 2024, Art. no. 120246, https://doi.org/10.1016/j.ins.2024.120246.

[23] J. Wu, T. Xu, T. Zhou, X. Chen, N. Zhang, and H. Hu, "Feature-Based Spectrum Sensing of NOMA System for Cognitive IoT Networks," *IEEE Internet of Things Journal*, vol. 10, no. 1, pp. 801–814, Jan. 2023, https://doi.org/10.1109/JIOT.2022.3204441.

[24] L. Lv, J. Chen, Q. Ni, Z. Ding, and H. Jiang, "Cognitive Non-Orthogonal Multiple Access with Cooperative Relaying: A New Wireless Frontier for 5G Spectrum Sharing," *IEEE Communications Magazine*, vol. 56, no. 4, pp. 188–195, Apr. 2018, https://doi.org/10.1109/MCOM.2018.1700687.

[25] X. Wang, H. Zhang, K. J. Kim, Y. Tian, and A. Nallanathan, "Performance Analysis of Cooperative Aerial Base Station-Assisted Networks With Non-Orthogonal Multiple Access," *IEEE Transactions on Wireless Communications*, vol. 18, no. 12, pp. 5983–5999, Dec. 2019, https://doi.org/10.1109/TWC.2019.2941199.

[26] S. Gamal, M. Rihan, S. Hussin, A. Zaghloul, and A. A. Salem, "Multiple Access in Cognitive Radio Networks: From Orthogonal and Non-Orthogonal to Rate-Splitting," *IEEE Access*, vol. 9, pp. 95569–95584, 2021, https://doi.org/10.1109/ACCESS.2021.3095142.

[27] T. Balachander and M. B. M. Krishnan, "Efficient Utilization of Cooperative Spectrum Sensing (CSS) in Cognitive Radio Network (CRN) Using Non-orthogonal Multiple Access (NOMA)," *Wireless Personal Communications*, vol. 127, no. 3, pp. 2189–2210, Dec. 2022, https://doi.org/10.1007/s11277-021-08776-7.

[28] P. Dutta *et al.*, "Evaluating the Efficiency of Non-Orthogonal MU-MIMO Methods in Smart Cities Technologies & 5G Communication," *Sustainability*, vol. 15, no. 1, Dec. 2022, Art. no. 236, https://doi.org/10.3390/su15010236.

[29] V. B. Kumaravelu *et al.*, "Outage Probability Analysis and Transmit Power Optimization for Blind-Reconfigurable Intelligent Surface-

Assisted Non-Orthogonal Multiple Access Uplink," *Sustainability*, vol. 14, no. 20, Oct. 2022, Art. no. 13188, https://doi.org/10.3390/su142013188.

[30] A. Ghani, S. H. A. Naqvi, M. U. Ilyas, M. K. Khan, and A. Hassan, "Energy Efficiency in Multipath Rayleigh Faded Wireless Sensor Networks Using Collaborative Communication," *IEEE Access*, vol. 7, pp. 26558–26570, 2019, https://doi.org/10.1109/ACCESS.2019.2898565.

[31] E. Bjornson and L. Sanguinetti, "Rayleigh Fading Modeling and Channel Hardening for Reconfigurable Intelligent Surfaces," *IEEE Wireless Communications Letters*, vol. 10, no. 4, pp. 830–834, Apr. 2021, https://doi.org/10.1109/LWC.2020.3046107.

[32] S. Ahmed and S. Ameen, "5G Mobile Communication Performance Improvement with Cooperative-NOMA Optimization," *International Journal of Computing and Digital Systems*, vol. 16, no. 1, pp. 1603–1616, Oct. 2024, https://doi.org/10.12785/ijcds/1601119.

[33] M. Aldababsa, C. Goztepe, G. K. Kurt, and O. Kucur, "Bit Error Rate for NOMA Network," *IEEE Communications Letters*, vol. 24, no. 6, pp. 1188–1191, Jun. 2020, https://doi.org/10.1109/LCOMM.2020.2981024.

[34] V. Yatnalli, B. G. Shivaleelavathi, and K. L. Sudha, "Review of Inpainting Algorithms for Wireless Communication Application," *Engineering, Technology & Applied Science Research*, vol. 10, no. 3, pp. 5790–5795, Jun. 2020, https://doi.org/10.48084/etasr.3547.

[35] S. W. Qu, J. L. Li, and Q. Xue, "Bowtie Dipole Antenna With Wide Beamwidth for Base Station Application," *IEEE Antennas and Wireless Propagation Letters*, vol. 6, pp. 293–295, 2007, https://doi.org/10.1109/LAWP.2007.898543.